



HAL
open science

Seasonal and interannual variability of salinity in a large West-African lagoon (Nokoué Lagoon, Benin)

Victor Olaègbè Okpeitcha, Alexis Chaigneau, Yves Morel, Thomas Stieglitz, Yves Pomalegni, Zacharie Sohoun, Daouda Mama

► To cite this version:

Victor Olaègbè Okpeitcha, Alexis Chaigneau, Yves Morel, Thomas Stieglitz, Yves Pomalegni, et al.. Seasonal and interannual variability of salinity in a large West-African lagoon (Nokoué Lagoon, Benin). Estuarine and Coastal Marine Science, 2021, 10.1016/j.ecss.2021.107689 . hal-03368397

HAL Id: hal-03368397

<https://hal.science/hal-03368397>

Submitted on 6 Oct 2021

HAL is a multi-disciplinary open access archive for the deposit and dissemination of scientific research documents, whether they are published or not. The documents may come from teaching and research institutions in France or abroad, or from public or private research centers.

L'archive ouverte pluridisciplinaire **HAL**, est destinée au dépôt et à la diffusion de documents scientifiques de niveau recherche, publiés ou non, émanant des établissements d'enseignement et de recherche français ou étrangers, des laboratoires publics ou privés.

1 **Seasonal and interannual variability of salinity in a large West-African**
2 **lagoon (Nokoué Lagoon, Benin)**

3
4 **Victor Olaègbè OKPEITCHA^{1,2,3,*}, Alexis CHAIGNEAU^{4,3,2}, Yves MOREL⁴, Thomas**
5 **STIEGLITZ⁵, Yves POMALEGNI², Zacharie SOHOU^{3,6}, Daouda MAMA¹**

6
7 ¹ Laboratoire d'Hydrologie Appliquée (LHA), Institut National de l'Eau (INE), African
8 Centre of Excellence for Water and Sanitation (C2EA), Université d'Abomey Calavi, Bénin

9 ² International Chair in Mathematical Physics and Applications (ICMPA–UNESCO
10 Chair)/University of Abomey- Calavi, Cotonou, Benin

11 ³ Institut de Recherches Halieutiques et Océanologiques du Bénin (IRHOB), Cotonou, Benin,

12 ⁴ Laboratoire d'Études en Géophysique et Océanographie Spatiale (LEGOS), Université de
13 Toulouse, CNES, CNRS, IRD, UPS, Toulouse, France

14 ⁵ Aix-Marseille Université, CNRS, IRD, INRAE, Coll France, CEREGE, Aix-en-Provence,
15 France

16 ⁶ Département de Zoologie, Faculté des Sciences et Techniques (FAST/UAC), Bénin

17
18
19
20
21
22
23
24
25 ***Corresponding author : Victor Olaègbè OKPEITCHA , vokpeitcha@gmail.com**

26 **Abstract**

27 Nokoué Lagoon in the South of Benin is a large intermittent coastal water body in
28 West Africa, which supports one of the largest inland fisheries of the region. The seasonal and
29 interannual variability of its salinity was studied, based on 3 years of monthly surveys (Dec
30 2017 - Dec 2020). This dataset allows us to identify fine-scale salinity structures and to better
31 understand the salinization/desalinization processes at seasonal scales. During the rainy
32 season from May to November, under the influence of large freshwater inflows from the
33 rivers on its northern shores, the lagoon desalinizes to a salinity of zero in October-November.
34 During the dry season from December to April, under the effect of the ocean tide, Nokoué
35 lagoon becomes progressively saltier, reaching typical salinities of ~25 in April. On average,
36 the Nokoué lagoon is saltier in its southwestern part and fresher towards the river's mouths.
37 Vertical salinity stratification is largest in December at the beginning of the main dry season.
38 The lagoon displays a very marked interannual variation with mean surface (bottom,
39 respectively) salinity of 25 (25) in April 2018 and 2020, respectively, against 16 (18) in April
40 2019. In the absence of river inflow data, a box model shows that the average salinity of the
41 lagoon is very sensitive to small changes in river inflow (or discharge), with observed
42 interannual differences in salinity induced by small variations of $10\text{-}15\text{ m}^3\text{ s}^{-1}$ in inflow during
43 the dry season. During the salinization phase, the model suggests that ~30% of the seawater
44 entering the lagoon during flood-tides remains trapped and enhances the Nokoué lagoon
45 salinity. This model also indicates that a complete desalinization of the lagoon occurs for river
46 inflow greater than $\sim 50\text{-}60\text{ m}^3\text{ s}^{-1}$. The general mixing time scale of the lagoon is of 30-40
47 days.

48

49 **Keywords:** Salinity; tropical lagoon; Nokoué lagoon; seasonal and interannual variations;
50 stratification; box model.

51 1. Introduction

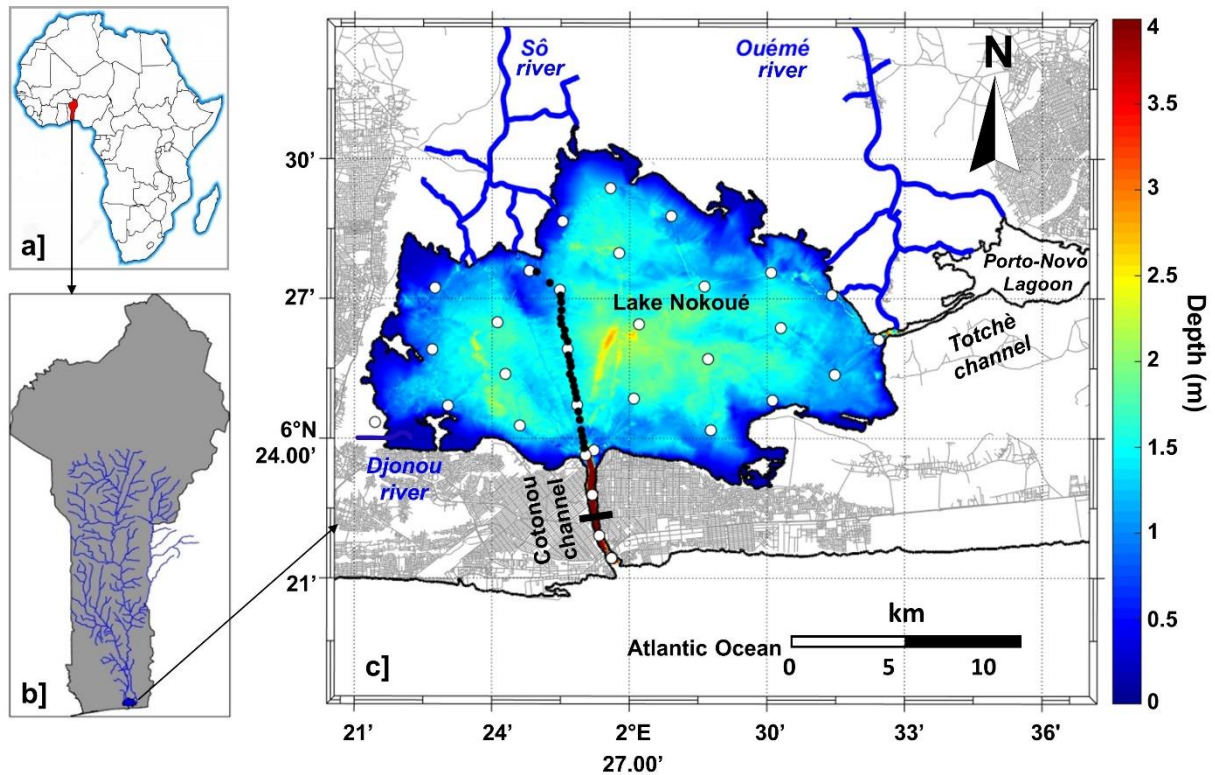
52 Lake Nokoué is located in South Benin (Fig. 1) between 6.33°N and 6.50°N and
53 2.33°E and 2.58°E. It extends over a maximum of ~11 km from South to North, and of ~20
54 km from West to East, covering an area of ~150 km² during low-water periods (Gadel and
55 Texier, 1986; Le Barbé et al., 1993). The lake is the largest body of water in Benin (Lalèyè et
56 al., 2003; Le Barbé et al., 1993) and the most productive in West Africa in terms of fish
57 resources (Badahoui et al., 2009; Gnohossou et al., 2013). Exploited by ~40000 fishermen, it
58 is the largest contributor to Benin's continental fisheries and thus contributes to food security
59 and socio-economic development. Lake Nokoué is subject to strong anthropogenic pressures.
60 Indeed, it not only hosts the largest lacustrine villages of West Africa (Djihouessi and Aina,
61 2018; Yehouenou et al., 2013) but is also surrounded by the largest cities of South Benin with
62 a population exceeding 1.5 million inhabitants (Gnohossou, 2006). Lake Nokoué is also part
63 of the Lagos (Nigeria) - Accra (Ghana) urban corridor made up of more than 2000 urban
64 agglomerations totalizing 30 million people today with a future projection of 50 million
65 inhabitants by 2050 (Choplin, 2019; Moriconi-Ebrard et al., 2016).

66 Lake Nokoué lies in a transition zone between the large catchment areas of the Ouémé
67 River in the north-east and the Sô River in the north-west, and the Atlantic Ocean, with which
68 it communicates through the 4.5 km long and ~300 m wide artificial Cotonou channel (Le
69 Barbé et al., 1993; Mama et al., 2011) (Figure 1). As a result of its permanent connection with
70 the Atlantic Ocean since construction of the channel, the previously unconnected 'Lake'
71 Nokoué (as it is still known in colloquial language) is today an extensive lagoon and is thus
72 hereinafter referred as Nokoué Lagoon. **Nokoué Lagoon also communicates in its western part
73 with the small Djonou River (a few meters wide and a few kilometers long) and in the east
74 with the Porto-Novo lagoon via the Totchè canal (Fig. 1), but they have little effect on the**

75 dynamics of Nokoué Lagoon (Texier et al., 1980; Le Barbé et al., 1993; Chaigneau et al.,
76 2021).

77 In Northern Benin, where the Ouémé River originates, the climate is tropical,
78 characterized by a single rainy season that extends from April to October, with maximum
79 rainfall in August and September (Gadel and Texier, 1986; N'Tcha M'Po et al., 2017;
80 Djihouessi and Aina, 2018). In the south, the climate is sub-equatorial and characterized by
81 two rainy seasons: a long rainy season that extends from April-May to July and a short season
82 that extends from September to November (Gadel and Texier, 1986; Djihouessi and Aina,
83 2018). During the short rainy season of South Benin, which coincides with the rainy season in
84 North Benin, the Ouémé and Sô rivers are in flood and discharge a large amount of fresh
85 water into Nokoué lagoon (Gadel and Texier, 1986; Djihouessi and Aina, 2018). The
86 maximum discharge into the lagoon between September and November is badly known
87 (rivers not regularly gauged in the coastal region), but some studies reported maximum river
88 fluxes varying, depending on authors, from $\sim 400 \text{ m}^3 \text{ s}^{-1}$ (Le Barbé et al., 1993; Djihouessi and
89 Aina, 2018) to more than $1000 \text{ m}^3 \text{ s}^{-1}$ (Lawin et al., 2019). The mean water level in the
90 lagoon, which is of $\sim 1.3 \text{ m}$ in dry season (Figure 1c), increases by up to $\sim 90 \text{ cm}$ during river
91 floods to reach an average value of $\sim 2.20 \text{ m}$ (Chaigneau et al., 2021). In contrast, the period
92 from December to April corresponds to the dry season in southern Benin, during which river
93 flow is minimal (a few tens of $\text{m}^3 \text{ s}^{-1}$) and the lagoon depth decreases to an average of 1.30 m
94 (Lalèyè et al., 2003; Niyonkuru and Lalèyè, 2010; Chaigneau et al., 2021; see also Fig. 1c).

95



96
 97 **Fig. 1.** Location of Nokoué lagoon (Benin) and hydrographic stations carried out between December 2017 and
 98 December 2020. a) Benin location in West-Africa. b) Hydrographic network of the Sô and Ouémé catchments in
 99 Benin; c) White dots represent the 31 CTD stations occupied monthly; black dots represent the 24 additional
 100 CTD stations occupied monthly in December 2017 and between February and December 2018; color shading
 101 represents the bathymetry during low water season. Black line across the Cotonou channel represents the
 102 repetitive cross-section occupied for ADCP measurements.

103

104 One of the key parameters of estuarine and lagoon environments is salinity, which greatly
 105 conditions the composition and structuring of ecosystems (Attrill, 2002). The salinity of
 106 Nokoué lagoon and its spatial and temporal variations are induced at first order by the
 107 exchange of fresh water from the rivers (mainly Sô and Ouémé) and seawater entering the
 108 lagoon via the Cotonou channel under the effect of the ocean tide (Le Barbé et al., 1993;
 109 Mama, 2010; Zandagba et al., 2016b). **From numerical simulations, typical tidal inflows and**
 110 **outflows in the Cotonou channel have been estimated to 400-1000 m³ s⁻¹, depending on the**
 111 **considered tidal period (neap or spring tides) and hydrological season (dry or wet) (Zandagba**

112 [et al., 2016b](#)). During high-water periods (September to November), Nokoué lagoon is filled
113 with fresh water and has zero salinity (Djihouessi and Aina, 2018; Mama et al., 2011;
114 Zandagba et al., 2016b). In contrast, during low-water periods the lagoon gradually becomes
115 saltier and salinity varies from 28 North of the Cotonou channel, to 5 close to the river mouths
116 (Djihouessi and Aina, 2018; Mama, 2010; Mama et al., 2011; Zandagba et al., 2016a).
117 Nokoué lagoon is therefore subject to significant variations in salinity on seasonal scales,
118 which impacts the composition and distribution of the ecosystem from planktonic species or
119 macroinvertebrates (Adandedjan et al., 2017; Le Barbé et al., 1993; Odountan et al., 2019) to
120 fish (Lalèyè et al., 2003). Seasonal variations of salinity in Nokoué lagoon are therefore very
121 important for ecosystem structuring but can also contribute to the salinization of the
122 underlying aquifer which is used to supply drinking water to the cities of Porto-Novo and
123 Cotonou (Alassane et al., 2015; Dovonou and Boukari, 2014). Salinization of the lagoon
124 during low-water periods also contributes to the periodic reduction of water hyacinth cover, a
125 prolific invasive plant present in large and increasing quantities during freshwater periods
126 (Mama, 2010; Mama et al., 2011).

127 Although salinity variations in Nokoué lagoon have been previously described at seasonal
128 scales (Djihouessi and Aina, 2018; Mama et al., 2011; Zandagba et al., 2016a), a thorough
129 analysis is still lacking and the data used in these previous studies present some limitations.
130 First, observations of salinity variations were discussed based on a limited number (3-5) of
131 sampling stations within the lagoon (Gnohossou, 2006; Lalèyè et al., 2003), followed by
132 studies which included 10-20 stations (Adandedjan et al., 2017; Djihouessi and Aina, 2018;
133 Zandagba et al., 2016a). Second, in all these studies, data were systematically acquired during
134 a limited period of time of one (Gnohossou, 2006; Lalèyè et al., 2003; Zandagba et al., 2016a)
135 or two years (Mama et al., 2011), and the frequency of acquisition varied from monthly
136 observations to only few field campaigns per year. Third, the vertical salinity structure and

137 stratification were barely discussed since salinity data were mainly acquired at the water
138 surface. Finally, among these 4 studies, only Djihouessi and Aina (2018) show spatial maps of
139 surface salinity allowing to identify frontal structures and horizontal salinity gradients.

140 In this study, based on 3 years of salinity data (2018-2020) acquired during 37 monthly
141 surveys, the seasonal and interannual variability of both the surface and bottom salinity in
142 Nokoué lagoon are examined. Monthly maps, together with high-resolution north-south
143 sections realized across the lagoon allow us to highlight fine-scale salinity structures and
144 better understand the salinization/desalinization processes that take place at the beginning of
145 the low- and high-water periods. In the absence of river inflow data, a simple box model is
146 further used to improve our understanding of the observed salinity changes.

147

148 **2. Data and methods**

149 Between December 2017 and December 2020, physical parameters of Nokoué lagoon
150 and the Cotonou channel were sampled in monthly intervals. During each survey, 31 vertical
151 temperature and salinity profiles were acquired using a Conductivity Temperature Depth
152 (CTD) probe (Valeport MIDAS CTD+ 300) deployed from the surface to the bottom (white
153 dots in Figure 1b). In December 2017 and between February and December 2018, high spatial
154 resolution north-south sections were also recorded between the Cotonou channel and the
155 mouth of the Sô River (Fig. 1b). These sections consisted of 24 additional hydrographic
156 stations in 250 m intervals, allowing us to document and monitor the monthly evolution of the
157 salt front and vertical stratification across the main (hydrological) axis of the lagoon.

158 The CTD acquisition frequency was 8 Hz and the parameters were recorded every 0.1
159 dbar (~10 cm) between the surface and the bottom, which the depth typically varies between
160 0.5 m and 2.5 m (Figure 1c). Only the descent CTD profiles were used. For each monthly
161 survey, salinity data from the 31 stations were spatially interpolated onto a regular grid of

162 ~100 m x 100 m resolution, using an objective interpolation scheme (Bretherton et al., 1976;
163 McIntosh, 1990; Wong et al., 2003). Note that salinity was measured using the Practical
164 Salinity Scale, with no units (see Millero, 1993, and UNESCO recommendations, 1985).

165 In order to interpret the observed salinity variations between 2018 and 2020,
166 exchanges of water between the Atlantic Ocean and the lagoon were monitored across the
167 Cotonou channel (see black line in Fig. 1c) at monthly intervals between August 2019 and
168 December 2020, using an acoustic Doppler current profiler (ADCP Teledyne RDI WorkHorse
169 1200-kHz), mounted on the side of a small wooden boat. Vertical profiles of velocity data
170 were collected at 1s intervals using WinRiver II software (RDI Teledyne) with GPS
171 positioning and bottom-tracking. For each transect, the total inflow-outflow transport across
172 the Cotonou channel was calculated by integrating velocity profiles throughout the wet cross-
173 section. Among the 17 monthly ADCP field campaigns, we only retained the ones collected
174 over more than 12 hours, providing inflow-outflow transport estimates during entire semi-
175 diurnal tidal cycles. **Since we are interested in estimating these transports during the**
176 **salinization period when the lagoon's water-level is relatively low and river inflow relatively**
177 **weak (see below and Section 4.1), we also excluded the 6 ADCP campaigns realized in**
178 **September-November of 2019 and 2020, when the river outflows were high.** Each of the 10
179 **ADCP** field campaigns retained in this study consisted of 100-200 repetitive cross-sections
180 that were occupied during 12-25 h.

181 Together with a box model, this ADCP dataset is used in Section 4.1 to estimate the
182 fraction of seawater that enters the lagoon during flood-tide and remains trapped within the
183 lagoon. In order to relate the tidal flow variations observed in the Cotonou channel from
184 ADCP data, to the tidal amplitude in the offshore ocean, we used **tide elevations (amplitude**
185 **and phase)** computed from the last Finite Elements Solution for ocean tide (FES2014) on a
186 $1/16^\circ \times 1/16^\circ$ grid (<http://www.aviso.altimetry.fr/en/data/products/auxiliary-products/global->

187 tide-fes.html) (Carrere et al. 2016; Lyard et al. 2020). Sea-level anomaly timeseries were
188 reconstructed off Cotonou using the 34 tidal constituents (amplitudes and phases) computed
189 from FES2014, and tidal amplitudes were then extracted from this timeseries for each of the
190 10 ADCP field campaigns.

191 We also used the Climate Hazards group Infrared Precipitation with Stations (CHIRPS)
192 dataset (<https://data.chc.ucsb.edu/products/CHIRPS-2.0/>). This gridded product consists to
193 rainfall estimates from blended rain gauge and satellite observations (Funk et al., 2015).
194 Terrestrial precipitation estimates are distributed on a $0.05^\circ \times 0.05^\circ$ longitude/latitude grid and
195 are available at daily to annual timeseries. We here used the decadal product, consisting of
196 precipitation data every 10 days from January 2018 to December of 2020.

197

198 **3. Results**

199 **3.1. Spatiotemporal variability of surface salinity**

200 Figure 2a shows the monthly variability of surface salinity in Nokoué lagoon since
201 December 2017, illustrating considerable seasonal variations. After a complete flushing of the
202 lagoon in the main wet season, freshwater inflow is greatly reduced at the beginning of the
203 main dry season in December, and seawater begins to enter the lagoon under the effect of the
204 tide through the Cotonou channel. This results in saline intrusion first observed in the west of
205 the lagoon. From January to April 2018, the lagoon is in a low-water period and gradually
206 becomes saltier. Salinity is consistently highest near the mouth of the channel, and lowest
207 close to the mouths of the rivers Sô (North-West), Ouémé (East-North-East) and Djonou
208 (South-West). From May to August 2018, the lagoon desalinizes rapidly and reaches very low
209 salinity values in July-August, at the end of the main rainy season in southern Benin. During

210 this period, the western part of the lagoon remains saltier than the east. This salinity difference
211 between the West and the East of the lagoon is ~8 in June-July and ~4 in August. During the
212 flood period (September to November), the lagoon is almost entirely fresh. Its salinity is
213 almost 0 during this period, and a substantial freshwater inflow inhibits any salt water
214 intrusion from the ocean. In December 2018, the main dry season begins once again: seawater
215 begins to penetrate into the lagoon again and a new cycle of salinization and desalination
216 begins.

217 Seasonal salinity variations exhibit regular patterns during the 3-year study period
218 (2018-2020) (Fig. 2a). Each year, from January to March-April, a gradual increase in salinity
219 is observed, reaching maximum values in April. The south/south-west of the lagoon is
220 systematically saltier, while the lowest salinity values systematically observed at the mouths
221 of the Sô, Ouémé and Djonou rivers. From May to August, the lagoon becomes desalinated
222 and a marked salinity gradient appears between the West and the East of the lagoon. From
223 September to November, the surface of the lagoon is entirely filled with fresh water.

224 Despite the overall regular patterns, an interannual variability is evident. While the
225 surface salinity values observed at the end of the low-water period in April 2018 and April
226 2020 are very similar, the overall salinity in April 2019 is significantly lower, in particular in
227 the East of the lagoon during the entire low-water period. The maximum observed salinity
228 value in April 2019 was 22, while it was 28 in April 2018 and 2020. Similarly, the minimum
229 salinity value observed at the mouth of the Ouémé River during the same month was ~20 in
230 2018 and 2020, and only 6 in 2019. Other differences can be observed on these maps. For
231 instance, the months of July-August were slightly saltier in 2018 than the following years,
232 whereas September and November 2020 were also saltier than in 2018 and 2019. More
233 noticeable, December 2019 was much less salty than December 2017, 2018 and 2020.

234

235 **3.2. Spatiotemporal variability of bottom salinity and lagoon**

236 **stratification**

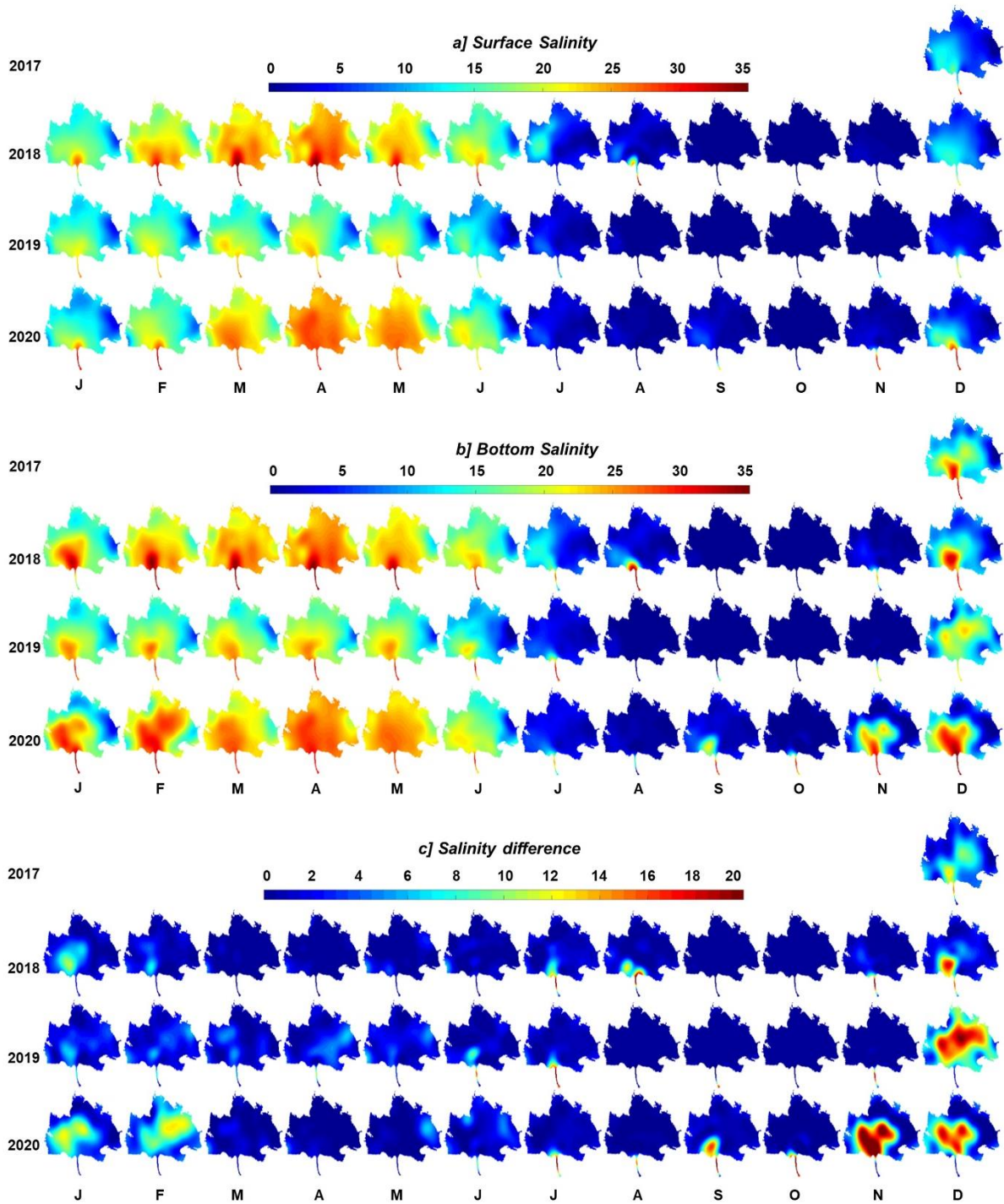
237 Figure 2b shows monthly variations of salinity at the bottom of the lagoon, typically
238 varying from 0.5 m to 2.5 m in depth depending on the station (see also Fig. 1c) and the
239 season. Overall, the salinity variations are comparable to those observed at the surface. The
240 onset of a saline intrusion is observed in December. From January to April, the intrusion
241 intensifies, with high salinity values observed at the end of the dry season (March-April).
242 From May onwards, the salinity at the bottom decreases until it reaches very low values in
243 July-August with a tendency to be saltier at the south-west of the lagoon. During the flood
244 period between September and November, the lagoon bottom is fresh, except in 2020 when
245 the saline intrusion started earlier in November. An interannual variability similar to that at
246 the surface is observed.

247 To investigate the vertical stratification, we consider the salinity difference between
248 the bottom and the surface as a measure of the vertical stratification in this very shallow
249 lagoon (Fig. 2c).

250 From January to February 2018, the stratification gradually decreases. From March to
251 June 2018, the salinity is vertically homogeneous. In July-August 2018, at the end of the main
252 wet season in Cotonou, there is a slight increase of stratification, still in the southwest of the
253 lagoon, but of less intensity than in December-January. In September-November, the lagoon
254 is fresh from the surface to the bottom and thus no vertical stratification present (Fig. 2c).

255 In January-February 2019, the vertical stratification is less than in 2018 (Fig 2c). This
256 relatively weaker stratification, associated with mean salinity differences of 2- 4 between the
257 bottom and the surface, but locally reaching more than 10, continues from February to May
258 2019. In 2019, salinity becomes homogeneous vertically only during the flood period between
259 August and November. In December 2019, stratification reaches a maximum with salinity

260 differences of 15-18 between the surface and the bottom over most of the lagoon. This very
261 strong stratification is maintained at the beginning of 2020 and then rapidly decreases as in
262 2018. In 2020, a pulse of high stratification was observed in September close to the Cotonou
263 channel, and the salinization of the lagoon at the bottom began earlier in November than in
264 other years (Figs. 2b-c). In contrast to December 2018, the maximum vertical stratification
265 observed in December 2017, 2019 and 2020 is not only located in the southwest but extends
266 over most of the lagoon. However, it remains very low at the mouths of the rivers compared
267 to the whole lagoon.



268

269 **Fig. 2.** Monthly variation in the Nokoué lagoon between December 2017 and December 2020 of a) surface
 270 salinity, b) bottom salinity and c) vertical salinity stratification. The stratification is here defined as the salinity
 271 difference between the bottom and the surface.

272

273

274 Note that stratification also depends on temperature distribution. At seasonal scale, the water
275 temperature varies from 26-28°C from June to October, to 31-32°C in March-April (not
276 shown). In September-November, during high-water period, when the lake is desalinated,
277 temperature differences between the surface and the bottom are maximum and can reach
278 1.5°C. During the rest of the year, vertical temperature differences are less than 0.5°C, but
279 lagoon temperature is subject to a relatively strong diurnal cycle of ~2°C, due to surface
280 heating by solar insolation. As horizontal and vertical temperature variations are significantly
281 weaker than salinity variations, we here consider only salinity variations in order to assess the
282 water column's vertical structure.

283

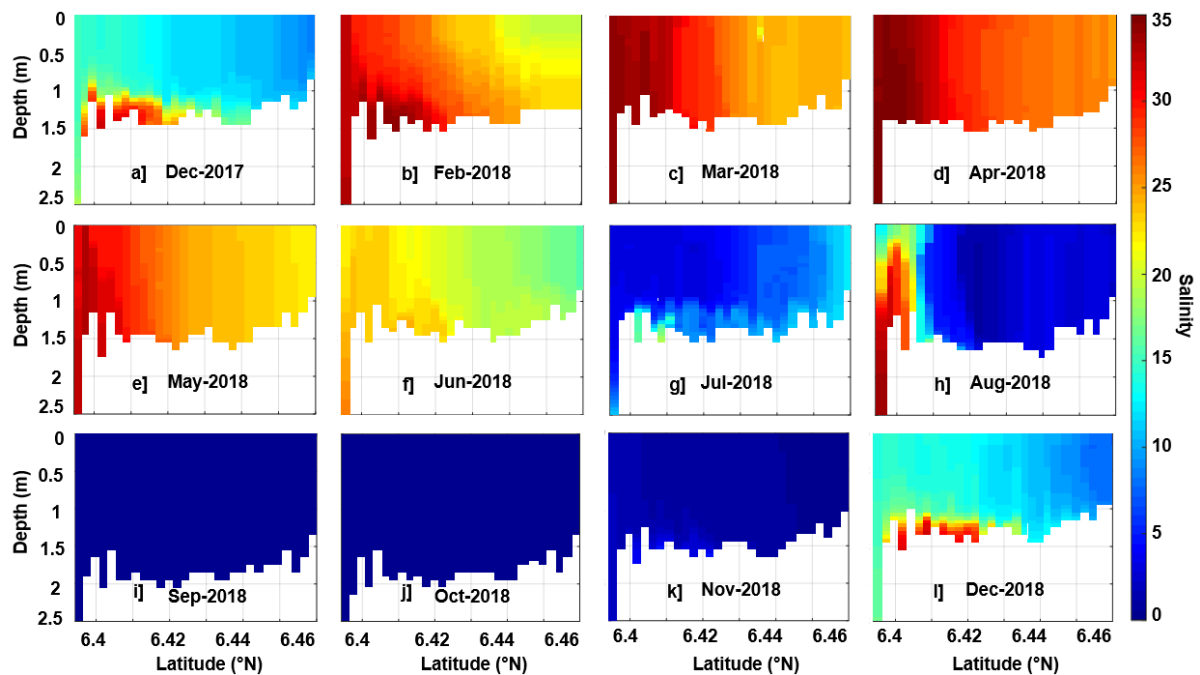
284 **3.3. High spatial resolution of the salt-wedge**

285 The high-resolution salinity sections recorded between the south and north of the
286 lagoon clearly show that the salinity exhibits a classical wedge-shaped distribution at the
287 beginning of the salinization and desalination periods (Fig. 3). This salt-wedge characteristic
288 is related to the presence of gravity currents associated with the difference in density between
289 fresh and salt water, and of weak vertical mixing despite the shallow depth (Fig. 1c) of the
290 lagoon. In December 2017, a highly saline bottom layer was observed in the south of the
291 lagoon with salinities of around 30 reaching latitude 6.42°N. In this region, the difference in
292 salinity between the bottom and the surface was about 15. North of latitude 6.42°N, salinity
293 drops considerably throughout the water column and stratification weakens northward. To the
294 north of the section, near the mouth of the Sô river, the water column is relatively
295 homogeneous and desalinated, with salinity differences of ~2 between the bottom and the
296 surface. In February 2018, the saline intrusion has intensified and extends to the North of the
297 lagoon, but the salinity difference between the bottom and the surface has been reduced and is
298 only ~5 South of latitude 6.42°N.

299 In March-April 2020, the salt-wedge has disappeared, and the water column is
300 homogeneously salty between the surface and the bottom. Salinity decreases from the
301 entrance of the channel (~35) to the mouth of the Sô river where salinities of around 25 are
302 observed at this period of the year. In May-June, salinity decreases over the entire water
303 column and the inflow of water from the Sô pushes the salinity front southwards. A
304 stratification begins to reappear between 6.41°N and 6.43°N again in the form of a weak salt-
305 wedge (bottom-surface salinity differences ~3).

306 In July 2018, the section is mostly filled with relatively fresh water (salinity values <
307 12) but lenses of salt water are still present on the bottom. Somewhat counter-intuitive,
308 salinity was also higher close to the Sô River than further South during this period. This is due
309 to the recirculation of a lens of saltier water observed in the south-west of the lagoon and
310 which flows northeastward along the northern shoreline of the lagoon (Figs. 2a-b). In August
311 2018, North of 6.41°N, salinity is vertically homogeneous and the lagoon is almost
312 desalinated (salinity values < 4). However, seawater penetrates from the South, and a very
313 strong salinity front is formed with a difference in salinity between the bottom and the surface
314 of about 10 (see also Fig. 2c).

315 From September to November, no stratification is observed along the South-North
316 section. As described above, the entire water column is homogeneous and filled with fresh
317 water and the lagoon reaches its highest water level, with values of more than 2 m.



318
 319 *Fig. 3. Monthly evolution of the salinity along the high-resolution section occupied in the lagoon Nokoué*
 320 *between December 2017 (a) and from February 2018 (b) to December 2018 (l). This South-North section*
 321 *crosses the lagoon from the entrance of the Cotonou channel to the mouth of the Sô river (see Fig.1c for the*
 322 *location of the transect).*

323

3.4. Interannual variability of the lagoon average salinity

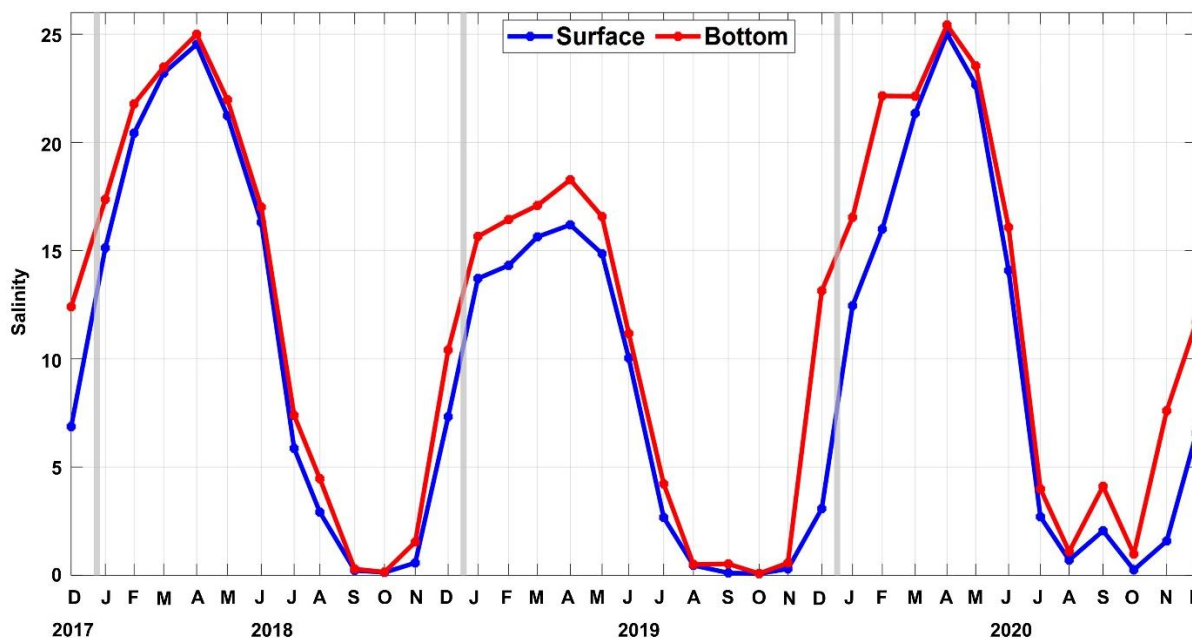
324

325 Surface and bottom salinity averaged over the lagoon exhibits large seasonal and
 326 interannual variations (Figure 4). Salinity increases rapidly from January to April, both at the
 327 surface and at the bottom, with maximum values observed in April. Salinity then decreases
 328 significantly from May to August during the main rainy season in South Benin, reaching zero
 329 values in September-November during the flood.

330 The annual maximum in surface and bottom salinity is significantly lower in April
 331 2019 than in April 2018 and 2020. In September 2020, the lagoon was slightly saltier than at
 332 the same period in 2018 and 2019, with average salinity values of ~2 at the surface and ~4 at
 333 the bottom. In 2020, the flooding (increased river inflow) was delayed compared to previous
 334 years, which favored the entry of seawater into the lagoon via the Cotonou channel in

335 September. In the same year, the saltwater intrusion started earlier in November in contrast to
 336 other years when the intrusion started in December.

337



338

339 *Fig. 4. Interannual variation of average surface and bottom salinity in the Nokoué lagoon between December*
 340 *2017 and December 2020. Data from the Cotonou channel were excluded.*

341

342 4. Discussion

343 In agreement with previous studies (Djihouessi and Aina, 2018; Mama, 2010; Mama
 344 et al., 2011; Zandagba et al., 2016a), our results show that the lagoon becomes saltier from
 345 December to April and then desalinates rapidly during the rainy seasons from May to
 346 November. Our study further shows that the salinization process of Nokoué lagoon begins in
 347 December, first at the bottom and southwest of the lagoon where a salt-wedge structure is
 348 observed. The salinization then spreads towards the northeast and the lagoon mixes vertically
 349 to become vertically homogeneous. Typical for coastal environments, the tide plays an
 350 important role during the salinization period as it regulates the exchange of waters with the
 351 ocean. Similarly, from May, the lagoon begins to desalinate first from the Northeast before

352 this desalination gradually reaches the Southwest which remains saltier. Desalination is
353 complete and the lagoon is filled with freshwater typically from August to November.

354 At first order, the average salinity of the lagoon results from a balance between i) the
355 exchange of water between the ocean and the lagoon due to tides, and ii) the inflow of fresh
356 water by the rivers. Thus, from the observed spatio-temporal salinity distributions, several
357 questions at the scale of the Nokoué lagoon arise, namely:

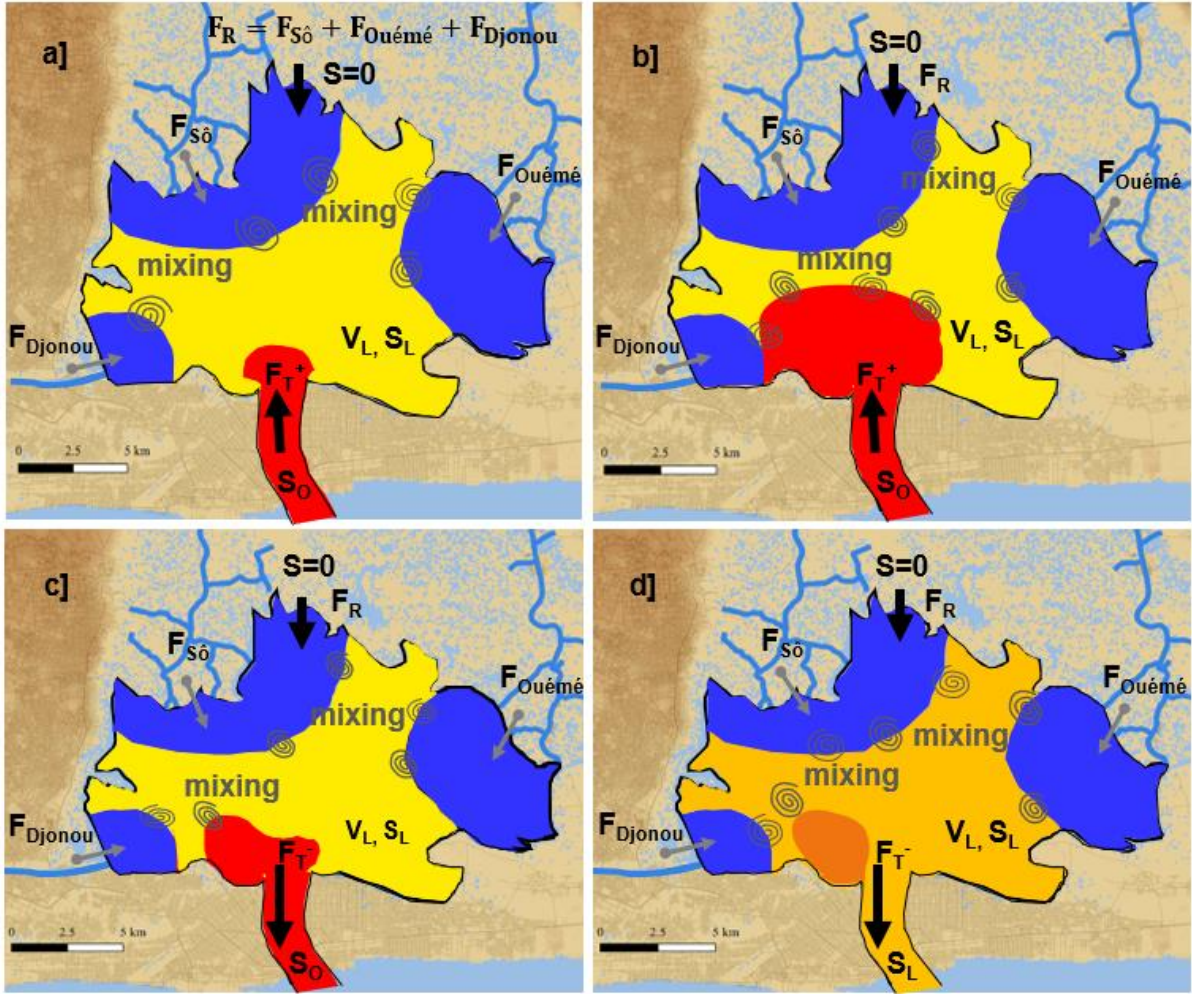
- 358 i. what is the order of magnitude of the river inflow that is required to explain such
359 strong salinization/desalinization with average salinities varying between 0 and
360 25?
- 361 ii. what is the fraction of seawater that is trapped and mixed into the lagoon during
362 each tidal cycle, in order to reach the high salinity levels observed during the dry
363 season?
- 364 iii. what process can explain the observed salinity difference between the dry season
365 of 2019 (salinity of ~16) and of 2018 and 2020 (salinity of ~25)?
- 366 iv. Finally, at local scale, what process is responsible for the observed salinity
367 gradient between the northeast and the southwest of the lagoon?

368 Unfortunately, because the Sô and Ouémé rivers are not regularly gauged, simultaneous river
369 discharge and salinity data are not available for the study period. Climatological historical
370 estimates indicate a total freshwater input to the lagoon that varies on average from a few tens
371 of $\text{m}^3 \text{s}^{-1}$ from December to July and that reach $\sim 800 \text{ m}^3 \text{ s}^{-1}$ between September and November
372 (Chaigneau et al., 2021). Similarly, continuous and long-term monitoring of freshwater and
373 saltwater exchanges between the lagoon and the ocean in the Cotonou Channel is not
374 available. Thus, to address the above questions, we use a simple box model.

375

376 **4.1. Key drivers of the lagoon salinity dynamics from a box model**

377 In order to better understand the salinity dynamics and to estimate important
378 parameters for the salt cycle, we use a simple conceptual box model similar to the *tidal prism*
379 model (de Miranda et al., 2017; Rynne et al., 2016). Figure 5 illustrates the exchange of water
380 in the lagoon for both tidal phases (flow and ebb tides) when river outflows are relatively
381 weak and seawater can penetrate the lagoon. During flood tide (Figs. 5a-b), we assume that
382 only seawater, of salinity S_0 , enters the lagoon with an average inflow F_T^+ . A fraction of this
383 seawater mixes with fresher lagoon water, probably in the southwest part of the basin, and
384 remains in the lagoon. During ebb tide (Figs. 5c-d), the mean outflow (F_T^-) transports i) a
385 fraction $(1 - \delta)$ of oceanic water which remains close to the mouth at the end of the flood tide
386 (Fig. 5c), and ii) a fraction δ of lagoon water of salinity S_L (Fig. 5d). Thus, δ represents the
387 fraction of oceanic water that remains in the lagoon during the tidal cycle. Simultaneously
388 during the whole tidal cycle, a continuous constant inflow of fresh water (F_R) by the rivers
389 ($F_{S\acute{o}}$, $F_{O\acute{u}\acute{e}m\acute{e}}$, F_{Djonou}) mixes with the lagoon water.



390

391 *Fig. 5. Conceptual model of the effects of tides on the salinity of the Nokoué lagoon. a) Beginning of the flood-*
 392 *tidal b) End of the flood-tide. c) Beginning of the ebb-tide. d) End of the ebb-tide. S_0 and S_L correspond to the*
 393 *lagoon and ocean salinity, respectively; V_L is volume of the lagoon; F_R is the river discharge whereas F_T^+ (F_T^- ,*
 394 *respectively) corresponds to the inflow (outflow) during flood (ebb) tide.*

395 Thus, during flood tide of duration T (for a semi-diurnal tide, $T \sim 21600$ s), volume
 396 (V_L) and salt (S_L) conservation within the lagoon can be written as:

$$397 \quad V_L(t_0 + T) = V_L(t_0) + F_T^+ T + F_R T \quad (1)$$

$$398 \quad V_L(t_0 + T) S_L(t_0 + T) = V_L(t_0) S_L(t_0) + F_T^+ S_0 T \quad (2)$$

399 And during the ebb-tide, the mass balance equations are:

$$400 \quad V_L(t_0 + 2T) = V_L(t_0 + T) + F_T^- T + F_R T \quad (3)$$

401 $V_L(t_0 + 2T) S_L(t_0 + 2T) = V_L(t_0 + T) S_L(t_0 + T) + \delta F_T^- S_L(t_0 + T) T + (1 - \delta) F_T^- S_O T$ (4)

402 Considering that the volume of the lagoon remains constant over a complete tidal
 403 cycle ($V_L(t_0 + 2T) = V_L(t_0)$), the total balance over the entire tidal cycle can then be
 404 written as:

405 $F_T^+ + F_T^- + 2F_R = 0$ (5)

406 $\frac{S_L(t_0+2T)-S_L(t_0)}{2T} = -\frac{S_L(t_0+T)-S_L^{eq}}{\tau}$ (6)

407 with

408 $\tau = -\frac{2V_L(t_0)}{\delta F_T^-}$ (7)

409 $S_L^{eq} = \left(1 + \frac{2F_R}{\delta F_T^-}\right) S_O$ (8)

410 **τ can be interpreted as the timescale of the transient salinization phase.**

411 In steady state, S_L^{eq} corresponds to the value reached by the salinity of the lagoon,
 412 which depends on the freshwater discharge F_R and the fraction of seawater that permanently
 413 remains in the lagoon. Note that for a sufficiently strong river inflow ($F_R > \frac{-\delta F_T^-}{2}$), the salinity
 414 in the lagoon becomes zero (because S_L^{eq} can not be negative). In transient regime, the
 415 variation of salinity is controlled by the coefficient τ , which depends only on the tidal outflow
 416 and the volume of the lagoon. Considering that the parameters defining τ and S_L^{eq} are constant
 417 during the transient regime, equation (6) leads to:

418 $S_L(t_0 + t) = S_L^{eq} + (S_L(t_0) - S_L^{eq})e^{-t/\tau}$ (9)

419 We now apply this model to the time series of observed average lagoon salinity (Fig.
 420 4). Considering S_L^{eq} , the salinity at steady state reached in April ($S_L^{eq} \sim 25$ in 2018 and 2020,
 421 and $S_L^{eq} \sim 16$ in 2019), and $S_L(t_0)$, the salinity at the beginning of the transient period in
 422 November-December, we can easily estimate the timescale τ from Eq. (9) as:

423
$$\tau = \frac{t}{-\log\left(\frac{S_L(t_0+t)-S_L^{eq}}{S_L(t_0)-S_L^{eq}}\right)}$$
 (10)

424 Fitting this to our dataset leads to an estimate of $\tau = 30\text{-}40$ days. Considering Eq. (7) and (8),
 425 and given the volume of the lagoon in the low water season ($V_L(t_0) \approx 1.5 \cdot 10^8 \text{ m}^3$) and the
 426 ocean salinity ($S_O \approx 35$), one can estimate the mean river discharge into the lagoon of $F_R =$
 427 $\left(1 - \frac{S_L^{eq}}{S_O}\right) \frac{V_L(t_0)}{\tau} \approx 25 - 30 \text{ m}^3 \text{ s}^{-1}$ during the dry season of 2019 and of $10\text{-}15 \text{ m}^3 \text{ s}^{-1}$ during
 428 the dry season of 2018 and 2020. Note however, that a clear salinity plateau was not observed
 429 during 2018 and 2020, suggesting that we probably underestimate the equilibrium value of
 430 salinity and slightly overestimate the river discharge for these 2 years.

431 Using inflow-outflow transports inferred for each of the 10 ADCP field campaigns
 432 between August 2019 and December 2020 (see Section 2), the mean outflow discharge
 433 observed during ebb-tides (F_T^-) varied between $-200 \text{ m}^3 \text{ s}^{-1}$ for neap tides (weak tidal
 434 amplitudes) to $-500 \text{ m}^3 \text{ s}^{-1}$ for spring tides (high tidal amplitudes) (Fig. 6). Thus, considering a
 435 timescale $\tau = 30\text{-}40$ days, during which the mean outflow discharge F_T^- is on average of -350
 436 $\text{m}^3 \text{ s}^{-1}$ (Fig. 6) we can estimate from Eq. (7) that:

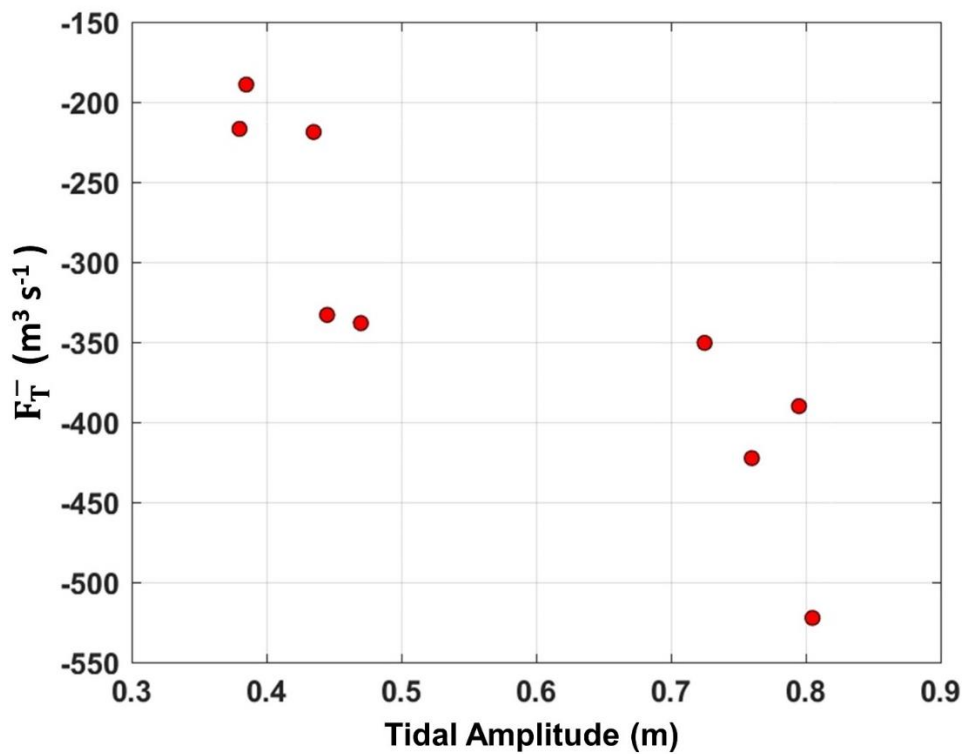
437
$$\delta = \frac{-2 V_L(t_0)}{\tau F_T^-} \approx 0.3$$

438 During the transient phase of salinization, and depending on the tide intensity, we thus
 439 estimate that a fraction of 30% of seawater entering the lagoon during flood-tide remains
 440 trapped and mixes with the fresher local water, progressively enhancing the salinity of the
 441 lagoon.

442 As noted above, the lagoon becomes totally desalinated when the river flow F_R
 443 becomes higher than $\frac{-\delta F_T^-}{2}$. Thus, using the values obtained above, the critical river inflow
 444 above which no salt can penetrate and the lagoon remains fresh is $\sim 50\text{-}60 \text{ m}^3 \text{ s}^{-1}$. Another

445 interesting way of interpreting the critical condition above which the lagoon is entirely
 446 desalinated is when the residence time in the lagoon ($T_{res} = \frac{V_L}{F_R}$) is below the timescale of the
 447 salinization phase ($\tau = 2 \frac{V_L}{\delta F_T^-}$). Overall, the simple box model suggests that in dry season, the
 448 salinity of Nokoué lagoon drastically depends on the river and groundwater discharges to the
 449 lagoon. Salinity can indeed range from 0 to 35 for inflow varying respectively from 50-60 to 0
 450 $\text{m}^3 \text{s}^{-1}$. So weak variations ($\sim 10 \text{ m}^3 \text{ s}^{-1}$) of the river discharge during the dry season can lead to
 451 very different salinities.

452



453

454 **Fig. 6.** Mean outflow transports (F_T^-) during ebb tides as a function of tidal amplitude in the offshore ocean. F_T^-
 455 have been estimated from the 10 ADCP field campaigns realized between August 2019 and December 2020 in
 456 Cotonou channel, whereas tidal amplitudes have been estimated from FES2014.

457

458

4.2. Estimate of the baroclinic effects

In section 3.3 we argued that the salt wedge is a sign of an important role of baroclinic effects for the penetration of salinity into the lagoon. Baroclinic effects are often neglected when modeling shallow lagoon and it is thus important to estimate this effect in the present case. To do so, we neglect all other processes (tide and river flux) and evaluate the flux associated with the baroclinic pressure gradient associated with the salinity difference between the ocean and the lagoon (Fig. 7). At the beginning of the dry season, the lagoon is fresh and the ocean salinity is $S_o \sim 35$. This is associated with a density difference $\Delta\rho \sim 26 \text{ kg.m}^{-3}$ between the ocean and the lagoon. Assuming the lagoon remains fresh, this generates a baroclinic pressure gradient between the ocean and the lagoon increasing from 0 at the surface to a maximum of $\sim \Delta\rho g h / L$ (see Fig. 7), where $g = 9.81 \text{ m s}^{-2}$ is the Earth gravity, $L \sim 4000 \text{ m}$ the channel length and $h \sim 1.3 \text{ m}$ the mean lagoon depth.

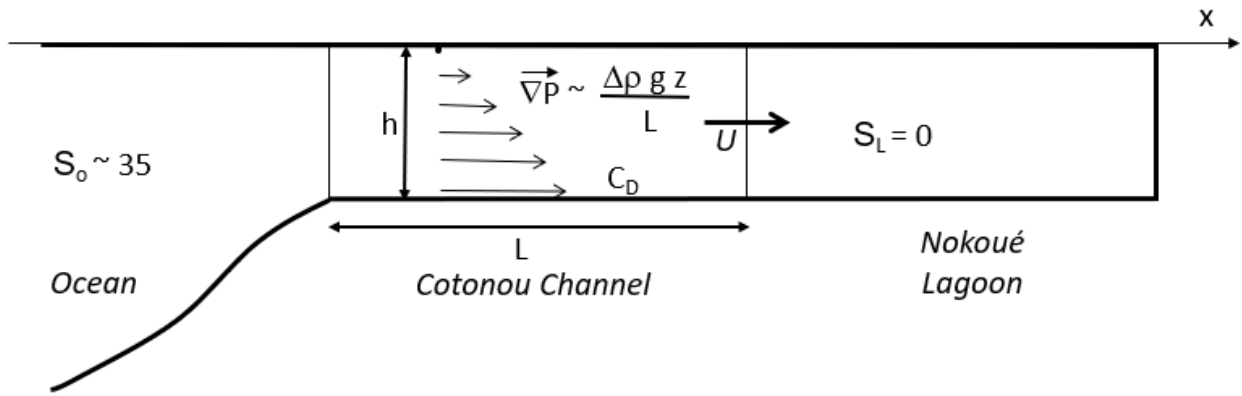


Fig. 7. Schematic (vertical cross section along the channel) of the configuration to evaluate the baroclinic effects associated with the salinity gradient between the ocean and the lagoon.

To evaluate the velocity field U associated with this pressure gradient, we follow Stigebrandt (1980) and assume it is equilibrated at first order by the bottom friction in the channel (Fig. 7) which can be expressed as

478
$$\nabla P = \frac{\Delta \rho g z}{L} \sim \rho C_D \frac{U^2}{h}$$

479 where $C_D \sim 0.004$ is the bottom friction coefficient. This gives an evaluation of the velocity
 480 field associated with the salinity gradient. Integrating the velocity profile from the surface to
 481 depth h and multiplying by the lagoon breadth $l \sim 280$ m, we get the mean transport
 482 associated with baroclinic effects:

483
$$T = \frac{2}{3} \sqrt{\frac{\Delta \rho g}{\rho C_D L}} h^2 l \sim 40 \text{ m}^3 \cdot \text{s}^{-1}$$

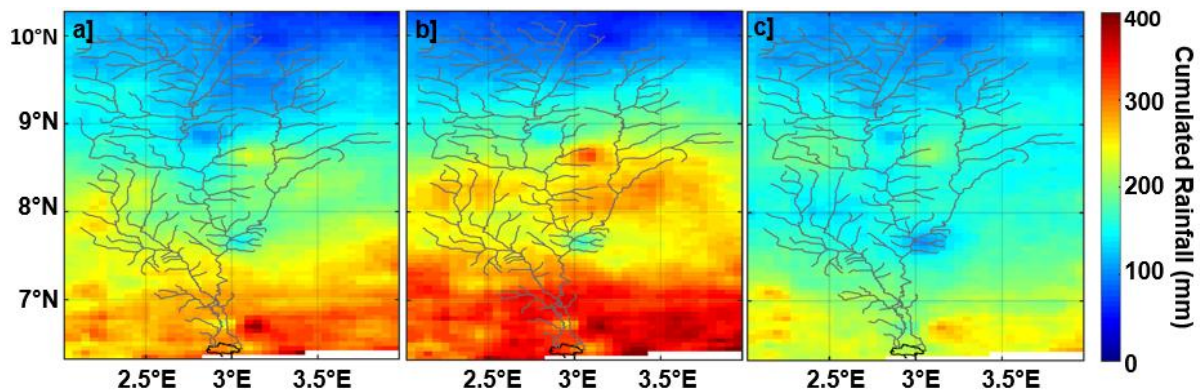
484 Interestingly, it is close to the critical river flux above which the lagoon will be entirely fresh
 485 ($\sim 50\text{-}60 \text{ m}^3 \text{ s}^{-1}$). The latter evaluation is a crude estimate, but it indicates that the fraction of
 486 the salinity flux entering the lagoon during the transient regime and associated with baroclinic
 487 effects is not negligible and should be considered in realistic models of the Nokoué lagoon.

488

489 **4.3. Interannual variability in dry season lagoon salinity**

490 To explain the observed interannual differences in dry season maximum salinity, the
 491 box model suggests that the river discharge must have been twice as large in 2019 ($25\text{-}30 \text{ m}^3$
 492 s^{-1}) as in 2018 or 2020 ($10\text{-}15 \text{ m}^3 \text{ s}^{-1}$). Hydrological data of the river discharge close to the
 493 coast is not available (not monitored). We therefore use CHIRPS-2.0 precipitation data (Funk
 494 et al., 2015) to confirm the most plausible cause of the reduced salinization observed in 2019
 495 i.e. a different rainfall regime in 2019. Figure 8 shows the cumulated rainfall observed
 496 between December and April for the 3 years (2018-2020). This Figure shows that rainfall was
 497 much more abundant in the dry season of 2019 compared to 2018 and 2020, more particularly
 498 in the southern part of the Ouémé catchment and over the Nokoué lagoon (Fig. 8). Over these
 499 5-month periods, the cumulated precipitations that fell within the Ouémé and Sô catchment

500 basins were of ~165 mm in 2018, ~200 mm in 2019 and ~150 mm in 2020. The higher
 501 cumulated precipitation in 2019 must have led to a higher freshwater discharge into the
 502 lagoon and is thus likely responsible for the lower salinity values observed from January to
 503 April 2019. During this period, the lagoon was also ~5-10 cm higher than during the dry
 504 season of 2018 and 2020 (Chaigneau et al., 2020), again suggesting a greater supply of fresh
 505 water in 2019, as already indicated by both the box model and precipitation data. Note that
 506 from the cumulated precipitations (Fig. 8), the beginning of 2020 was likely the driest season
 507 of this 3-year period. However, salinity in 2020 was similar to 2018 (Figs. 2a-b, 4),
 508 suggesting that other processes may also affect the lagoon salinity and mixing such as wind,
 509 waves, or changes in the morphology of the Cotonou channel mouth that can modify salt
 510 fluxes.



511
 512 **Fig. 8.** Cumulated rainfall (December-April) over the Ouémé basin catchment in a) 2018, b) 2019, and c) 2020.
 513 The hydrographic network of the Sô and Ouémé catchments is shown in gray, whereas as the Nokoué lagoon is
 514 delimited in black.

515 Finally, at local scale, the salinity dataset has highlighted a mean salinity gradient
 516 between the North-East (minimum salinity) and the South-West (maximum salinity) of the
 517 lagoon (Figs. 2a-b). Intuitively, this stronger desalinization at the eastern part of the lagoon,
 518 may be due to a stronger discharge of the Ouémé River compared to the Sô River.
 519 Unfortunately, due to the lack of hydrological measurements in the catchment basins, the

520 relative importance of the freshwater discharges from the Sô and Ouémé remains unclear.
521 Previous studies suggested that during the dry season (December – April), the Sô discharge
522 would be much higher ($\sim 30\text{-}40 \text{ m}^3 \text{ s}^{-1}$) than the Ouémé outflow ($\sim 5\text{-}15 \text{ m}^3 \text{ s}^{-1}$) mainly due to
523 an excess of groundwater discharge into the Sô (Djihouessi and Aina, 2018; Mama et al.,
524 2011; Zandagba et al., 2016b). In contrast, during the wet season, these authors indicate a
525 stronger discharge of the Ouémé ($230\text{-}340 \text{ m}^3 \text{ s}^{-1}$) compared to the Sô ($120\text{-}200 \text{ m}^3 \text{ s}^{-1}$), due to
526 a much larger catchment area of the Ouémé River. Thus, our results, based on salinity
527 observations only, seem to partly contradict these previous studies, since a stronger
528 desalinization is generally observed at the mouth of the Ouémé River all year long and in
529 particular during the dry season (Fig. 2a).

530

531 **5. Conclusion**

532 Monthly salinity observations spanning three years documented the seasonal and
533 interannual variations of the salinity and vertical stratification in Nokoué lagoon, with
534 significantly greater freshwater influence observed in 2019.

535 Using a simple box model, we estimated that these interannual differences - consistent
536 with observed rainfall variations over the lagoon's catchment - can be induced by weak
537 variations of $10\text{-}15 \text{ m}^3 \text{ s}^{-1}$ in the river discharge during the dry season. In dry season, we
538 estimated that around 30% of the seawater entering the lagoon by tides, mixes with the fresher
539 lagoon's water and enhances its salinity. This relatively simple model also suggests that the
540 lagoon is completely desalinated for a river discharge greater than $\sim 50\text{-}60 \text{ m}^3 \text{ s}^{-1}$. The model
541 also provided a useful characteristic time scale $\tau \sim 30\text{-}40$ days for the salinization of the
542 lagoon. Estimates for the desalination are similar so that the general mixing time scale of the
543 lagoon is 30-40 days.

544 These results show that the salinity of Nokoué lagoon is very sensitive to small
545 changes in river's discharge. Additional data would be required to improve the understanding
546 of the main forcing mechanisms involved in the observed spatio-temporal salinity variations
547 of the lagoon (e.g. freshwater discharge, evaporation, wind and wave mixing, change in the
548 morphology of the Cotonou channel...). Overall, the salinity data and results obtained in this
549 study provide a useful baseline for ecosystem management purposes or to anticipate the
550 response of this important West-African lagoon under climate-change scenarios.

551

552 **Acknowledgements**

553 Field campaigns and instrumentation were chiefly supported by IRD, with contributions from
554 ANR @RAction chair medLOC (ANR-14-ACHN-0007-01 – T. Stieglitz). V. OKPEITCHA
555 was funded by OmiDelta project of the Embassy of the Kingdom of the Netherlands in Benin,
556 through a scholarship grant of the National Institute of Water (INE/UAC). This work is a
557 contribution to the « JEA1 SAFUME » project funded by IRD. Special thanks to the members
558 and crew participating to the monthly surveys, and in particular A. ASSOGBA, M.
559 BENOIST, and J. AZANKPO. Collaboration of Team 2/ODA-INE is also acknowledged.

560

561

562

563

564

565 **References**

- 566 Adandedjan, D., Makponse, E., Hinvi, L.C., Laleye, P., 2017. Données préliminaires sur la
567 diversité du zooplancton du lac Nokoué (Sud-Bénin). *J. Appl. Biosci.* 115, 11476–
568 11489. <https://doi.org/10.4314/jab.v115i1.7>.
- 569 Alassane, A., Trabelsi, R., Dovonon, L.F., Odeloui, D.J., Boukari, M., Zouari, K., Mama, D.,
570 2015. Chemical Evolution of the Continental Terminal Shallow Aquifer in the South of
571 Coastal Sedimentary Basin of Benin (West-Africa) Using Multivariate Factor Analysis.
572 *J. Water Resour. Prot.* 07, 496–515. <https://doi.org/10.4236/jwarp.2015.76040>.
- 573 Attrill, M.J., 2002. A testable linear model for diversity trends in estuaries. *J. Anim. Ecol.* 71,
574 262–269. <https://doi.org/10.1046/j.1365-2656.2002.00593.x>.
- 575 Badahoui, A., Fiogbe, E., Boko, M., 2009. Les causes de la dégradation du chenal de
576 Cotonou. *Int. J. Biol. Chem. Sci.* 3, 979–997. <https://doi.org/10.4314/ijbcs.v3i5.51077>.
- 577 Bretherton, F.P., Davis, R.E., Fandry, C.B., 1976. A technique for objective analysis and
578 design of oceanographic experiments applied to MODE-73. *Deep. Res. Oceanogr. Abstr.*
579 23, 559–582. [https://doi.org/10.1016/0011-7471\(76\)90001-2](https://doi.org/10.1016/0011-7471(76)90001-2).
- 580 Carrere, L., Lyard, F., Cancet, M., Guillot, A., and Picot, N. , 2016a. FES 2014, a new tidal
581 model – Validation results and perspectives for improvements, ESA Living Planet
582 Conference, Prague, Czech Republic.
- 583 Chaigneau A., Stieglitz T., Okpeitcha V., Assogba A., Sohou Z., Peugeot C., Morel Y., 2020.
584 Impact du changement global sur les systèmes lagunaires en Afrique de l’Ouest : le cas
585 du lac Nokoué au Bénin. *Météo et Climat Info* n°79 - Juillet 2020.
- 586 Chaigneau, A., Okpeitcha, V. O., Morel, Y., Stieglitz, T., Assogba, A., Benoist, M., Allamel,
587 P., Honfo, J., Awoulbang Sakpak, T. D., Rétif, F., Duhaut, T., Peugeot, C., Sohou Z.,
588 2021. From seasonal flood pulse to seiche: Multi-frequency water-level fluctuations in a
589 large shallow tropical lagoon (Nokoué Lagoon, Benin). *Estuarine Coastal and Shelf*

590 *Science, revised.*

591 Choplin, A., 2019. Produire la ville en Afrique de l'Ouest : le corridor urbain de Accra à
592 Lagos. *Inf. Geogr.* 83, 85. <https://doi.org/10.3917/lig.902.0085>.

593 de Miranda, L.B., Andutta, F.P., Kjerfve, B., Castro Filho, B.M. de, 2017. *Fundamentals of*
594 *Estuarine Physical Oceanography, Ocean Engineering & Oceanography*. Springer,
595 Singapore.

596 Djihouessi, M.B., Aina, M.P., 2018. A review of hydrodynamics and water quality of Lake
597 Nokoué: Current state of knowledge and prospects for further research. *Reg. Stud. Mar.*
598 *Sci.* 18, 57–67. <https://doi.org/10.1016/j.rsma.2018.01.002>

599 Dovonou, E.F., Boukari, M., 2014. *Gestion environnementale des aquifères superficiels au*
600 *sud-Bénin: Etat des lieux et mesures de protection*, Editions U. ed. Verlag.

601 Funk, C., Peterson, P., Landsfeld, M., Pedreros, D., Verdin, J., Shukla, S., Husak, G.,
602 Rowland, J., Harrison, L., Hoell, A., Michaelsen, J., 2015. The climate hazards infrared
603 precipitation with stations - A new environmental record for monitoring extremes. *Sci.*
604 *Data* 2, 150066. <https://doi.org/10.1038/sdata.2015.66>

605 Gadel, F., Texier, H., 1986. Distribution and nature of organic matter in recent sediments of
606 Lake Nokoué, Benin (West Africa). *Estuar. Coast. Shelf Sci.* 22, 767–784.
607 [https://doi.org/10.1016/0272-7714\(86\)90098-3](https://doi.org/10.1016/0272-7714(86)90098-3)

608 Gnohossou, P., 2006. *La faune benthique d'une lagune ouest Africaine (le lac Nokoué au*
609 *Bénin), diversité, abondance, variations temporelles et spatiales, place dans la chaîne*
610 *trophique*. Université de Toulouse > Institut National Polytechnique de Toulouse -
611 Toulouse INP (FRANCE).

612 Gnohossou, P., Lalèyè, P., Atachi, P., Magali, G., Villanueva, M., Moreau, J., 2013. Temporal
613 variations in the food habits of some fish species in Lake Nokoué, Benin. *African J.*
614 *Aquat. Sci.* 38, 43–47. <https://doi.org/10.2989/16085914.2013.792768>

615 Lalèyè, P., Niyonkuru, C., Moreau, J., Teugels, G.G., 2003. Spatial and seasonal distribution
616 of the ichthyofauna of lake nokoué, bénin, west africa. *African J. Aquat. Sci.* 28, 151–
617 161. <https://doi.org/10.2989/16085910309503779>

618 Le Barbé, L., Alé, G., Texier, H., Borel, Y., Gualde, R., 1993. Les ressources en eaux
619 superficielles de la République du Bénin, ORSTOM. ed, MONOGRAPHIES
620 HYDROLOGIQUES. Institut Français de Recherche Scientifique pour le
621 Développement en Coopération, Paris.

622 Lawin, A.E., Hounguè, R., N'Tcha M'Po, Y., Hounguè, N.R., Attogouinon, A., Afouda,
623 A.A., 2019. Mid-Century Climate Change Impacts on Ouémé River Discharge at Bonou
624 Outlet (Benin). *Hydrology*, 6 (72), <https://doi.org/10.3390/hydrology6030072>.

625 Lyard, F. H., Allain, D. J., Cancet, M., Carrere, L., and Picot, N. , 2020. FES2014 global
626 ocean tides atlas: design and performances, *Ocean Sciences Discussions*, 1–40,
627 <https://doi.org/10.5194/os-2020-96>.

628 Mama, D., 2010. Méthodologie et résultats du diagnostic de l'eutrophisation du lac Nokoué
629 (Bénin). Thèse. Université de Limoges.

630 Mama, D., Deluchat, V., Bowen, J., Chouti, W., Yao, B., Gnon, B., Baudu, M., 2011.
631 Caractérisation d'un système lagunaire en zone tropicale: Cas du lac nokoué (Bénin).
632 *Eur. J. Sci. Res.* 56, 516–528.

633 McIntosh, P.C., 1990. Oceanographic data interpolation: Objective analysis and splines. *J.*
634 *Geophys. Res.* 95, 13529. <https://doi.org/10.1029/jc095ic08p13529>

635 Millero, F. J., 1993. What is PSU? *Oceanography*, 6(3), 67.

636 Moriconi-Ebrard, F., Harre, D., Heinrigs, P., 2016. L'urbanisation des pays de l'Afrique de
637 l'Ouest 1950-2010 : Africapolis I, mise à jour 2015, Cahier de. ed. OCDE, Paris.

638 Niyonkuru, C., Lalèyè, P.A., 2010. Impact of acadja fisheries on fish assemblages in Lake
639 Nokoué, Benin, West Africa. *Knowl. Manag. Aquat. Ecosyst.* 5.

640 <https://doi.org/10.1051/kmae/2010033>

641 N'Tcha M'Po, Y., Lawin, E., Yao, B., Oyerinde, G., Attogouinon, A., Afouda, A., 2017.

642 Decreasing Past and Mid-Century Rainfall Indices over the Ouémé River Basin, Benin

643 (West Africa). *Climate* 5 (74).

644 Odountan, O.H., de Bisthoven, L.J., Koudenoukpo, C.Z., Abou, Y., 2019. Spatio-temporal

645 variation of environmental variables and aquatic macroinvertebrate assemblages in Lake

646 Nokoué, a RAMSAR site of Benin. *African J. Aquat. Sci.* 44, 219–231.

647 <https://doi.org/10.2989/16085914.2019.1629272>

648 Rynne, P., Reniers, A., van de Kreeke, J., MacMahan, J., 2016. The effect of tidal exchange

649 on residence time in a coastal embayment. *Estuar. Coast. Shelf Sci.* 172, 108–120.

650 <https://doi.org/10.1016/j.ecss.2016.02.001>.

651 *Stigebrandt, A., 1980. Some aspects of tidal interactions with fjord constrictions. Estuar.*

652 *Coast. Shelf Sci.* 11, 151-166.

653 *Texier, H., Colleuil, B., Profizi, J.P., Dossou, C., 1980. Le lac Nokoué, environnement du*

654 *domaine margino-littoral sud-béninois : bathymétrie, lithofaciès, salinité, mollusque et*

655 *peuplements végétaux. Bull. Inst. Géol. Bass. Aguit.. Bordeaux* 28, 115-142.

656 United Nations Educational, Scientific and Cultural Organization, 1985. The international

657 system of units (SI) in oceanography, UNESCO Technical papers, N°45, IAPSO Sci.

658 N°32, Paris, France.

659 Wong, A.P.S., Johnson, G.C., Owens, W.B., 2003. Delayed-mode calibration of autonomous

660 CTD profiling float salinity data by χ -S climatology. *J. Atmos. Ocean. Technol.* 20, 308–

661 318. [https://doi.org/10.1175/1520-0426\(2003\)020<0308:DMCOAC>2.0.CO;2](https://doi.org/10.1175/1520-0426(2003)020<0308:DMCOAC>2.0.CO;2)

662 Yehouenou, E.A.P., Adamou, R., Azehoun, P.J., Edorh, P.A., Ahoyo, T., 2013. Monitoring of

663 heavy metals in the complex “Nokoué lake - Cotonou and Porto-Novo lagoon”

664 ecosystem during three years in the Republic of Benin. *Res. J. Chem. Sci.* 3, 12–18.

665 Zandagba, J., Adandedji, F.M., Mama, D., Chabi, A., Afouda, A., 2016a. Assessment of the
666 Physico-Chemical Pollution of a Water Body in a Perspective of Integrated Water
667 Resource Management: Case Study of Nokoué Lake. *J. Environ. Prot.* (Irvine,. Calif).
668 07, 656–669. <https://doi.org/10.4236/jep.2016.75059>

669 Zandagba, J., Moussa, M., Obada, E., Afouda, A., 2016b. Hydrodynamic modeling of Nokoué
670 Lake in Benin. *Hydrology* 3, 44. <https://doi.org/10.3390/hydrology3040044>

671